Interatomic Coulombic electron capture

K. Gokhberg and L. S. Cederbaum

Theoretische Chemie, Physikalisch-Chemisches Institut, Universität Heidelberg, Im Neuenheimer Feld 229, D-69120 Heidelberg, Germany

(Received 28 July 2010; published 22 November 2010)

In a previous publication [K. Gokhberg and L. S. Cederbaum, J. Phys. B **42**, 231001 (2009)] we presented the interatomic Coulombic electron capture process—an efficient electron capture mechanism by atoms and ions in the presence of an environment. In the present work we derive and discuss the mechanism in detail. We demonstrate thereby that this mechanism belongs to a family of interatomic electron capture processes driven by electron correlation. In these processes the excess energy released in the capture event is transferred to the environment and used to ionize (or to excite) it. This family includes the processes where the capture is into the lowest or into an excited unoccupied orbital of an atom or ion and proceeds in step with the ionization (or excitation) of the environment, as well as the process where an intermediate autoionizing excited resonance state is formed in the capturing center which subsequently deexcites to a stable state transferring its excess energy to the environment. Detailed derivation of the asymptotic cross sections of these processes is presented. The derived expressions make clear that the environment assisted capture processes can be important for many systems. Illustrative examples are presented for a number of model systems for which the data needed to construct the various capture cross sections are available in the literature.

DOI: 10.1103/PhysRevA.82.052707 PACS number(s): 34.80.Lx, 52.20.Fs

I. INTRODUCTION

Capture of free electrons by atoms and ions is an elementary physical process of general interest. For the isolated in space atom or ion the only possibility to capture a slow electron is by photorecombination (PR) [1]. One can view this process as the inverse of photoionization or photodetachment. In a collision event, a free electron of energy ε is captured into the bound level of a species A forming A^-, while a photon is simultaneously emitted which carries away the excess energy. If the species A is neutral this process is commonly called radiative attachment, while if A is a positive ion the term radiative recombination is used. Both radiative attachment and radiative recombination are important in astrophysics [2,3], while radiative recombination is also very important in the physics of plasmas [4,5]. The photorecombination proceeds predominantly to the lowest unoccupied orbital of A producing the ground state of A^- [4,6]. If A is a positive ion, then as the energy of the incoming electron approaches an excitation energy of A it can be captured in a doubly excited resonance state of the compound system A^-. This state might stabilize by emitting a photon producing A^- in some excited state. The complete process is called dielectronic recombination [7,8] and is manifested in the photorecombination cross section as a number of peaks at the energies corresponding to the doubly excited resonances of A^- [4].

In the situation when A is not isolated but is embedded into the environment we have shown previously [9] that under certain conditions on the energy of the incoming electron the following interatomic process becomes possible. The electron is captured into the lowest unoccupied orbital of A while the energy released in the process is transferred to the neighboring atom B and used to ionize it [see Fig. 1(a) for a schematic representation]. Since this energy transfer is mediated through the electron-electron interaction, we called this process interatomic Coulombic electron capture (ICEC). We presented in Ref. [9] an analytical formula for the cross section of ICEC valid in the case of large interatomic distances between the capturing center A and the medium atom B. Applying this formula to a number of selected systems we have shown that ICEC is more probable than photorecombination for interatomic distances of the order of a few nanometers and transferred energies up to about 10 eV.

In this article we would like first to present and discuss the derivation of the ICEC cross section. The second purpose of this article is to discuss additional mechanisms of the environment assisted electron capture not mentioned in Ref. [9] and derive working equations for their cross sections. For example, we have seen in Ref. [9] that ICEC is enhanced if the energy transferred in the process becomes smaller. Therefore, unlike in the case of photorecombination, the probability of interatomic capture into excited unoccupied orbitals of A [represented pictorially in Fig. 1(b)], if energetically allowed, exceeds in general the capture into the lowest one. As the result one obtains in the final state A^- in an excited state. Another mechanism not mentioned in the original Letter and which we call dielectronic ICEC (dICEC) is the interatomic capture through the dielectronic resonances of A^-. In this process, the incoming electron having the energy in some narrow interval around a specific value corresponding to an autoionizing excited state of A^- is captured into a Rydberg or some other type of virtual orbital of A, while another, a "core" electron of A, is excited. The resulting resonance state of A^- can decay either into the dielectronic recombination channel by emitting a photon or into the dICEC channel by ionizing a neighbor [see a schematic representation of dICEC in Fig. 1(c)]. The latter interatomic decay mode belongs to the class of the resonant interatomic Coulombic decay (RICD) processes, whose properties have been previously studied both experimentally and theoretically [10–12]. For completeness we mention that the interatomic capture may proceed not through the ionization but through the excitation of the surrounding medium—a process one may call a resonant ICEC. Indeed, one such mechanism has been reported recently [13]. We discuss it briefly in the context of interatomic Coulombic processes and show its relation to the RICD process.

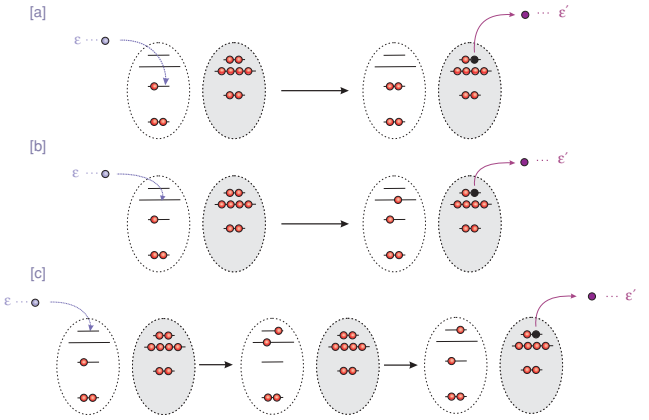

FIG. 1. (Color online) Schematic representation of different interatomic electron capture mechanisms discussed in the text. (a) ICEC; the incoming electron of energy ε is captured into the lowest unoccupied orbital of species A (empty oval), and the excess energy is transferred to a neighboring species B (shaded oval) and used to ionize it. (b) ICEC into excited virtual orbitals; the same as in (a) with the incoming electron captured into an excited unoccupied orbital of A. As is shown in the text the capture into an excited orbital, once allowed, will dominate the capture into the lowest unoccupied orbital. (c) dielectronic ICEC; in the first step the incoming electron is captured into an autoionizing state of $(A^-)^{**}$. In the second step this resonance decays by ionizing the neighbor B. For completeness we mention that the above processes may proceed not only through ionization but also through the excitation of the environment.

To demonstrate the efficiency of the interatomic capture compared with photorecombination and to show the dependence of the resulting cross sections on the electron energy and properties of the capturing center and the environment we consider several model systems. The criterion for their selection was the possibility to observe both ICEC and dICEC in each of them in order to compare the relative importance of these capture channels. Therefore, our choice was limited to systems for which one can find all necessary data in the literature. Since the latter include, in addition to relatively abundant ground-state photoionization cross sections, the relatively scarce excited-state photoionization cross sections, as well as the positions and widths of doubly excited resonances, the systems we have chosen are rather limited. We considered the interatomic capture by the following species: Ne^+ with Xe atoms or benzene (Bz) molecules forming the environment, He^+ in the presence of Ar and Bz, and Mg^+ in the presence of Br^-. We would like to stress that one can easily choose capturing centers and environments for which the cross sections are expected to be much larger than for noble gases discussed here.

The article is organized as follows. In the next section we discuss first the general aspects of the ICEC process. We proceed then to the derivation of the working asymptotic formulas for the ICEC and dICEC processes. The section concludes with a brief discussion of the resonant ICEC process. In the following section we illustrate the ICEC and dICEC mechanisms using the model systems mentioned above. In the last section we give the conclusions and outlook.

II. THEORY

A. ICEC

1. General considerations

We start the theoretical consideration of the ICEC process by looking at some of its general features. This process in the presence of one neighbor B can be symbolically represented by the following equation

$$e(\varepsilon) + A + B \rightarrow A^- + B^+ + e(\varepsilon'), \tag{1}$$

where ε and ε' are the kinetic energies of the incoming and outgoing electrons. A can be neutral or ionic atomic species, while B can be either an atom, a molecule, or an ionic species. Notwithstanding the charge state of A we will call it an atom throughout this article. We also assume that both A and B are initially in their ground states. For the moment we limit the discussion to the case of one neighbor B. The case of several neighbors will be considered later in the text.

If the energy of the target system in the initial state is E_{AB} and in the final state is $E_{A^-B^+}$, we can write the energy conservation condition as $\varepsilon + E_{AB} = \varepsilon' + E_{A^-B^+}$. The threshold kinetic energy of the incoming electron beyond which the interatomic capture process becomes energetically allowed is, therefore, given by $\varepsilon_t = E_{A^-B^+} - E_{AB}$. If the energy of the incoming electron exceeds the threshold, the ICEC process becomes possible. To find its cross section we apply the methods of the multichannel scattering theory [14]. In the in-channel the target AB is in the state $|\Phi_{AB}\rangle$. The corresponding N-electron antisymmetrized wave function can be designated as $\Phi_{AB}(\mathbf{r}_1, \ldots, \mathbf{r}_N)$, where the coordinates $\mathbf{r}_i$ include the spin variable. The scattering in-asymptote is given by

$$\langle \mathbf{r}|\mathbf{k}; \Phi_{AB}\rangle = \phi_{\mathbf{k}}(\mathbf{r}_0)\Phi_{AB}(\mathbf{r}_1, \ldots, \mathbf{r}_N), \tag{2}$$

where $\phi_{\mathbf{k}}(\mathbf{r}_0)$ is the wave vector normalized wave function of the free incoming electron with the wave number $\mathbf{k}$. In the out-channel the target is left in some state $|\Phi_{A^-B^+}\rangle$ while the outgoing electron is given by a wave with the wave vector $\mathbf{k}'$. The corresponding out-asymptote is given by

$$\langle \mathbf{r}|\mathbf{k}'; \Phi_{A^-B^+}\rangle = \phi_{\mathbf{k}'}(\mathbf{r}_0)\Phi_{A^-B^+}(\mathbf{r}_1, \ldots, \mathbf{r}_N). \tag{3}$$

We assume that the energy of the in state is E and the one of the out state is E', these energies being equal in a scattering process. The evolution of the in-asymptote into the out-asymptote is governed by the following Hamiltonian

$$\hat{H} = \hat{H}_{AB} + \hat{T}_0 + U = \hat{H}_0 + U, \tag{4}$$

where $\hat{H}_{AB}$ is the target Hamiltonian, $\hat{T}_0$ the kinetic energy operator of the free electron, and U is the scattering potential. The latter includes the repulsion between the free electron and the electrons in the target, and the attraction of the free electron to the nuclei A and B. Thus,

$$U = e^2 \sum_{i=1}^{N} r_{0i}^{-1} - e^2 \sum_{X=A,B} \frac{Z_X}{|\mathbf{r}_0 - \mathbf{R}_X|}. \tag{5}$$

The states entering the calculation are the so-called scattering states $|\mathbf{k}; \Phi_{AB}+\rangle$ and $|\mathbf{k}'; \Phi_{A^-B^+}-\rangle$, with the corresponding

$(N+1)$-electron wave functions given by

$$\langle \mathbf{r}|\mathbf{k};\Phi_{AB}+\rangle = \Phi^{+}_{\mathbf{k},AB}(\mathbf{r}_0;\mathbf{r}_1,\ldots,\mathbf{r}_N) \tag{6a}$$

$$\langle \mathbf{r}|\mathbf{k}';\Phi_{A^-B^+}-\rangle = \Phi^{-}_{\mathbf{k}',A^-B^+}(\mathbf{r}_0;\mathbf{r}_1,\ldots,\mathbf{r}_N). \tag{6b}$$

The semicolon separating the coordinates in the functions above indicates that the function is not yet antisymmetrized with respect to $\mathbf{r}_0$. The scattering states in Eqs. (6a) and (6b) are the eigenstates of the full Hamiltonian $\hat{H}$ with the energies E and E' respectively. They can be obtained from the in- and out-asymptotes using the Lippmann-Schwinger equations. Thus,

$$\begin{aligned}|\mathbf{k};\Phi_{AB}+\rangle &= |\mathbf{k};\Phi_{AB}\rangle + G(E+i0)U|\mathbf{k};\Phi_{AB}\rangle \\ &= |\mathbf{k};\Phi_{AB}\rangle + G^0(E+i0)U|\mathbf{k};\Phi_{AB}+\rangle \quad (7a)\\ |\mathbf{k}';\Phi_{A^-B^+}-\rangle &= |\mathbf{k}';\Phi_{A^-B^+}\rangle + G(E'-i0)U|\mathbf{k}';\Phi_{A^-B^+}\rangle \\ &= |\mathbf{k}';\Phi_{A^-B^+}\rangle + G^0(E'-i0)U|\mathbf{k}';\Phi_{A^-B^+}-\rangle, \quad (7b)\end{aligned}$$

where $G^0(E\pm i0)=(E-\hat{H}_0\pm i0)^{-1}$ and $G(E\pm i0)=(E-\hat{H}\pm i0)^{-1}$ are the Green's operators. The state in Eq. (7a) describes the state of the $(N+1)$-electron system which has evolved from the in-asymptote, while the state in Eq. (7b) is the state of the $(N+1)$-electron system which will evolve into the out-asymptote.

Since the incoming electron is indistinguishable from the electrons in the target one has to antisymmetrize the scattering states in Eqs. (6a) and (6b) with respect to $\mathbf{r}_0$. To do that we employ the Hermitian and idempotent operator

$$\Lambda_N = \frac{1}{N!}\sum_{\Pi}(-1)^{\eta}\Pi, \tag{8}$$

where Π is a permutation of N coordinates and η is the latter's parity. We antisymmetrize the states in Eqs. (6a) and (6b) by acting with $\sqrt{N+1}\Lambda_{N+1}$ on them. The S-matrix element corresponding to the transition of interest is given by [14,15]

$$S(\text{out}\leftarrow\text{in}) = (N+1)\langle \mathbf{k}';\Phi_{A^-B^+}-|\Lambda_{N+1}|\mathbf{k};\Phi_{AB}+\rangle. \tag{9}$$

Using the expression for the on-shell t matrix

$$S(\text{out}\leftarrow\text{in}) = -2\pi i\delta(E'-E)t(\text{out}\leftarrow\text{in}), \tag{10}$$

and the Eqs. (7a) and (7b) one obtains for the t matrix

$$\begin{aligned}t(\text{out}\leftarrow\text{in}) = &\int d\tau[\phi_{\mathbf{k}'}(\mathbf{r}_0)\Phi_{A^-B^+}(\mathbf{r}_1,\ldots,\mathbf{r}_N)]^* \\ &\times U\Phi^{+}_{\mathbf{k},AB}(\mathbf{r}_0;\mathbf{r}_1,\ldots,\mathbf{r}_N) \\ &+\sum_{i=1}^{N}(-1)^i\int d\tau[\phi_{\mathbf{k}'}(\mathbf{r}_0) \\ &\times\Phi_{A^-B^+}(\mathbf{r}_1,\ldots,\mathbf{r}_N)]^*U \\ &\times\Phi^{+}_{\mathbf{k},AB}(\mathbf{r}_i;\mathbf{r}_0,\mathbf{r}_1,\ldots,\mathbf{r}_{i-1},\mathbf{r}_{i+1}\ldots\mathbf{r}_N). \quad (11)\end{aligned}$$

This structure of the t matrix is due to the indistinguishability of the free electron from the electrons in the target. The first term gives the amplitude of the direct reaction, where the incoming and outgoing electrons are the same. The second term is the amplitude of the exchange reaction where one of the target's electrons goes away.

Once the t matrix is known the differential cross section can be found as

$$\frac{d\sigma(\mathbf{k}'\leftarrow\mathbf{k})}{d\Omega_{\mathbf{k}'}} = \frac{m_e^2}{(2\pi)^2\hbar^4}\frac{k'}{k}|t(\text{out}\leftarrow\text{in})|^2, \tag{12}$$

where the absolute values of the wave vectors of the initial and final states are connected by energy conservation. To obtain the total cross section for ICEC, the differential cross section is summed over all final states and averaged over all initial states at the energy $\varepsilon = k^2/2m_e$ giving

$$\sigma_{\text{ICEC}}(k) = \frac{1}{g_{\text{in}}}\sum_{\text{in,out}}\int\frac{d\Omega_{\mathbf{k}}}{4\pi}\int d\Omega_{\mathbf{k}'}\frac{d\sigma(\mathbf{k}'\leftarrow\mathbf{k})}{d\Omega_{\mathbf{k}'}}, \tag{13}$$

where g_{in} is the multiplicity of the initial state.

2. *Asymptotic formula for the ICEC cross section*

When the interatomic separation between A and B is large one can derive an analytical asymptotic expression for the t matrix and the cross section of ICEC. But before we proceed to finding this expression we would like to discuss the way to estimate the ICEC threshold as $R\to\infty$. Let $V_n^{(A)}$ stand for the binding energy of the excess electron by the atom A in the orbital n (electron affinity of A if A is a neutral atom and ionization potential of A^- if A is an ion). For convenience we shall call $V_n^{(A)}$ in the following the electron affinity of A. We designate by $V_i^{(B)}$ the energy needed to remove an electron from B and call it, for simplicity, the ionization potential of B even if B is not a neutral atom. At the limit of infinite separation between A and B it is easy to show that the ICEC threshold is given by $\varepsilon_t = V_i^{(B)} - V_n^{(A)}$, if $V_i^{(B)} \geqslant V_n^{(A)}$, and $\varepsilon_t = 0$ otherwise. For finite distances between the atoms, even large enough to make the orbital overlap between A and B insignificant, one might need to correct the value of the threshold. The change from the asymptotic value of the threshold energy is the most pronounced, if both the capturing center and its neighbor are charged either in the initial or the final state. It is the situation where the lowest-order corrections can be found trivially. We consider below some representative situations. Thus, if both A and B are neutral, then one obtains in the final state a positively and a negatively charged ion. Correcting for the attraction of the ions in the final state one obtains for the threshold $\varepsilon_t = V_i^{(B)} - V_n^{(A)} - e^2/R + O(1/R^2)$. In the case of doubly ionized A and neutral B correcting for the Coulomb repulsion of the two positive ions in the final state one obtains $\varepsilon_t = V_i^{(B)} - V_n^{(A)} + e^2/R + O(1/R^2)$.

Let us proceed to the derivation of the ICEC cross section. We start by remarking that as $R\to\infty$ one can distinguish between the electrons located on A and those located on B. Thus, the in-asymptote can be written as

$$\langle \mathbf{r}|\mathbf{k};\Phi_{\mathbf{AB}}\rangle = \phi_{\mathbf{k}}(\mathbf{r}_0)\Phi_A\left(\mathbf{r}_1,\ldots,\mathbf{r}_{N_A}\right)\Phi_B\left(\mathbf{r}_{N_A+1},\ldots,\mathbf{r}_N\right), \tag{14}$$

and for the out-asymptote one obtains

$$\begin{aligned}\langle \mathbf{r}|\mathbf{k}';\Phi_{A^-B^+}\rangle = &\Phi_{A^-}\left(\mathbf{r}_0,\mathbf{r}_1,\ldots,\mathbf{r}_{N_A}\right)\phi_{\mathbf{k}'}\left(\mathbf{r}_{N_A+1}\right) \\ &\times\Phi_{B^+}\left(\mathbf{r}_{N_A+2},\ldots,\mathbf{r}_N\right). \quad (15)\end{aligned}$$

We see that the outgoing electron in the out-asymptote comes from B. The process, where this electron is the incoming one or comes from A, would involve an electron transfer from B to A and have a negligible amplitude at large interatomic separation. The $(N+1)$-electron Hamiltonian can be represented in the in-channel as

$$\hat{H} = \hat{H}_A + \hat{H}_B + \hat{T}_0 + V_{\rm I}^{\alpha} + V_{\rm II}^{\alpha} = \hat{H}^{\alpha} + V^{\alpha}, \quad (16)$$

where $\hat{H}_A$, and $\hat{H}_B$ are the Hamiltonians of isolated A and B, $\hat{T}_0$ is the kinetic energy of the incoming electron. The sum of these three operators gives the channel Hamiltonian $\hat{H}^{\alpha}$, with the superscript α designating the in-channel. We divide the scattering potential into two components. The first term,

$$V_{\rm I}^{\alpha} = e^2 \sum_{i=1}^{N_A} r_{0i}^{-1} - \frac{Z_A e^2}{|\mathbf{r}_0 - \mathbf{R}_A|}, \quad (17)$$

is the interaction between the incoming electron and the atom A, while the second term,

$$V_{\rm II}^{\alpha} = e^2 \sum_{i=0}^{N_A} \sum_{j=N_A+1}^{N} r_{ij}^{-1} \quad (18)$$

contains the interaction between the electrons of A plus the incoming electron and the electrons of B. Analogously we write the Hamiltonian in the out-channel as

$$\hat{H} = \hat{H}_{A^-} + \hat{H}_{B^+} + \hat{T}_{N_A+1} + V_{\rm I}^{\beta} + V_{\rm II}^{\beta} = \hat{H}^{\beta} + V^{\beta}, \quad (19)$$

where $\hat{H}^{\beta}$ is the channel Hamiltonian with β designating the out-channel and the scattering potential given as

$$V_{\rm I}^{\beta} = e^2 \sum_{i=N_A+2}^{N} r_{(N_A+1)i}^{-1} - \frac{Z_B e^2}{|\mathbf{r}_{N_A+1} - \mathbf{R}_B|} \quad (20a)$$

$$V_{\rm II}^{\beta} = V_{\rm II}^{\alpha} \quad (20b)$$

The scattering states are now given by

$$|\mathbf{k}; \Phi_{AB}+\rangle = |\mathbf{k}; \Phi_A \Phi_B\rangle + G(E+i0) V^{\alpha} |\mathbf{k}; \Phi_A \Phi_B\rangle \quad (21a)$$

$$|\mathbf{k}'; \Phi_{A^-B^+}-\rangle = |\mathbf{k}'; \Phi_{A^-} \Phi_{B^+}\rangle + G(E'-i0) V^{\beta} |\mathbf{k}'; \Phi_{A^-} \Phi_{B^+}\rangle, \quad (21b)$$

The state in Eq. (21a) describes the incoming electron scattering off the atom A far from B. Thus, in what follows we have to antisymmetrize this state only with respect to the coordinates $\mathbf{r}_0, \mathbf{r}_1, \ldots, \mathbf{r}_{N_A}$. Similarly, the state in Eq. (21b) describes the electron leaving the atom B far from A, and one needs to antisymmetrize this state with respect to the coordinates $\mathbf{r}_{N_A+1}, \ldots, \mathbf{r}_N$. We designate the corresponding antisymmetrizers as $\sqrt{N_A+1}\Lambda_A$ and $\sqrt{N-N_A}\Lambda_B$. These antisymmetrizers commutate since they act on different sets of coordinates. Using this property we obtain for the S-matrix element

$$\begin{aligned} S(\text{out} \leftarrow \text{in}) &= \sqrt{N_A+1}\sqrt{N-N_A} \\ &\times \langle \mathbf{k}'; \Phi_{A^-} \Phi_{B^+} - |\Lambda_B \Lambda_A| \mathbf{k}; \Phi_A \Phi_B+\rangle \\ &= \sqrt{N_A+1}\sqrt{N-N_A} \\ &\times \langle \mathbf{k}'; \Phi_{A^-} \Phi_{B^+} - |\mathbf{k}; \Phi_A \Phi_B+\rangle. \end{aligned} \quad (22)$$

We use next the distorted-wave Born approximation [14] to calculate the t matrix. For this purpose we assume that the solution of the scattering problem is known exactly if $V_{\rm II}^{\alpha} = V_{\rm II}^{\beta} = 0$. Thus, in this case one obtains for the scattering states

$$|\mathbf{k}; \Phi_{AB}+_{\rm I}\rangle = |\mathbf{k}; \Phi_A+\rangle |\Phi_B\rangle \quad (23a)$$

$$|\mathbf{k}'; \Phi_{A^-B^+}-_{\rm I}\rangle = |\Phi_{A^-}\rangle |\mathbf{k}'; \Phi_{B^+}-\rangle, \quad (23b)$$

where the states $|\Phi_B\rangle$ and $|\Phi_{A^-}\rangle$ are the bound states of isolated B and A^-, while $|\mathbf{k}; \Phi_A+\rangle$ and $|\mathbf{k}'; \Phi_{B^+}-\rangle$ are the outgoing and ingoing scattering states of isolated A^- and B. Utilizing the states in Eqs. (23a) and (23b) and taking the potential $V_{\rm II}^{\beta}$ only to first order we obtain

$$\begin{aligned} t_{\rm DWBA}(\text{out} \leftarrow \text{in}) &= \sqrt{N_A+1}\sqrt{N-N_A} \\ &\times \langle \mathbf{k}'; \Phi_{A^-B^+} -_{\rm I} | V_{\rm II}^{\beta} | \mathbf{k}; \Phi_{AB}+_{\rm I}\rangle. \end{aligned} \quad (24)$$

Using the fact that $R \to \infty$ we apply the multipole expansion to the potential $V_{\rm II}^{\beta}$. Retaining only the leading term we obtain

$$V_{\rm II}^{\beta} = -\frac{1}{R^3} \sum_{m=-1}^{1} B_m \hat{D}_m^{(A)} \hat{D}_{-m}^{(B)}, \quad (25)$$

where $\hat{D}_A = e\sum_{i=0}^{N_A} r_m$ and $\hat{D}_B = e\sum_{i=N_A+1}^{N} r_m$ are dipole operators acting on the electrons located either on A or B and $B_0 = 2$, $B_{\pm 1} = 1$. Inserting Eq. (25) in Eq. (24) and using Eqs. (23a) and (23b) we finally obtain

$$\begin{aligned} t(\text{out} \leftarrow \text{in}) &= -\frac{1}{R^3} \sum_{m=-1}^{1} B_m \langle \Phi_{A^-} | \hat{D}_m^{(A)} | \mathbf{k}; \Phi_A+\rangle \\ &\times \langle \mathbf{k}'; \Phi_{B^+} - | \hat{D}_{-m}^{(B)} | \Phi_B\rangle, \end{aligned} \quad (26)$$

where the properly antisymmetrized scattering states of A^- and B are used. As we have noted above, the derived t matrix neglects all terms involving transfer of an electron from to A in the scattering event. This allows for an interpretation of the result in Eq. (26) as a *virtual photon* transfer, a model used in the framework of a related interatomic Coulombic processes [16,17]. Indeed, the amplitude of the complete process is a product of the amplitudes of the processes occurring on the isolated atoms, i.e., photorecombination and photoionization, connected to each other by the transfer of the virtual photon.

We introduce the t matrix in the form given in Eq. (26) into Eqs. (12) and (13). To facilitate the integration over $\Omega_{\mathbf{k}}$ and $\Omega_{\mathbf{k}'}$ one expands the plane waves in the initial and final states in terms of spherical waves (see Ref [1] for details). At large R the weight of the initial state $g_{\rm in} = 2 g_A g_B$, where g_A and g_B are the weights of the corresponding states of atoms A and B, respectively, while 2 corresponds to the spin multiplicity of the incoming electron. Using this value of $g_{\rm in}$ and the definitions of the cross sections for photoionization and photorecombination [1] we arrive at

$$\sigma_{\rm ICEC}(\varepsilon) = P(E_{\rm vph}, R) \sigma_{\rm PR}^{(A)}(\varepsilon), \quad (27)$$

where $\sigma_{\rm PR}^{(A)}(\varepsilon)$ is the cross section for photorecombination of A. The term

$$P(E_{\rm vph}, R) = \frac{3\hbar^4 c^4}{4\pi} \frac{\sigma_{\rm PI}^{(B)}(\varepsilon')}{R^6 E_{\rm vph}^4} \quad (28)$$

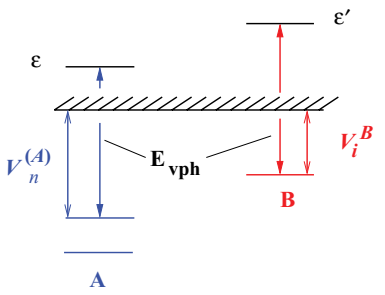

FIG. 2. (Color online) Schematic representation of the ICEC process and the parameters entering the asymptotic expressions for its cross sections. $V_n^{(A)}$ is the binding energy of the excess electron by the atom A in the orbital n. $V_i{}^B$ is the ionization potential of the neighbor, while ε and ε' are the energies of the incoming and outgoing electrons, respectively. $E_{\rm vph}$ denotes the energy of the virtual photon.

is a dimensionless coefficient, $E_{\rm vph} = V_n^{(A)} + \varepsilon$ is the energy of the virtual photon, and $\sigma_{\rm PI}^{(B)}(\varepsilon')$ is the photoionization cross section of B.[1] The ICEC process and the corresponding parameters are visualized in Figs. 1(a) and 2.

This expression allows us to compare the efficiencies of PR and ICEC for capturing a free electron of energy ε. If $P(E_{\rm vph}, R)$ is larger than unity, ICEC dominates over PR. The value of this coefficient is determined by three parameters: the distance R between A and its neighbor B, the energy $E_{\rm vph}$ of the virtual photon, and the photoionization cross section of B. $P(E_{\rm vph}, R)$ grows with decreasing R as does the interaction between the two transition dipoles which is proportional to R^{-6}. At a fixed interatomic distance the interatomic capture is likely to increase compared to the photorecombination as the virtual photon energy $E_{\rm vph}$ decreases. For instance, the value of $E_{\rm vph}$ decreases if, for a system with $V_n^{(A)} > V_i^{(B)}$, one finds a way to decrease $V_n^{(A)}$. This is achieved, for example, when the electron is captured into the higher energy virtual orbital of A resulting in the electronically excited A^- in the final state. Thus, the interatomic capture of the electron into orbitals other than the lowest unoccupied orbital of A may be more probable than the capture into the lowest unoccupied orbital, which is the exact opposite to what happens in photorecombination [4,6]. We discuss this capture mode more detailed in the next subsection. The value of the ICEC cross section also depends on the energies of the virtual photon and incoming electron through the photorecombination and photoionization cross sections. Since both of these cross sections tend to fall off fast with energy the optimal conditions for ICEC are realized when $V_n^{(A)} \approx V_i^{(B)}$ and the incoming electron is slow. Alternatively, choosing a neighbor which has a shape resonance in its photoionization cross section at the energies close to $E_{\rm vph}$ leads to the enhancement of the ICEC cross section.

The latter situation is often realized when B is a molecule which prompts the following consideration. If A is an atom and B is a molecule, their arrangement cannot be described by a single parameter R. The formulas in Eqs. (12), (13), and (26) used to derive the asymptotic expression of the ICEC cross section are completely general. However, in Eqs. (27), (28), and (33) for simplicity of presentation we averaged over possible orientations of B and used the corresponding averaged photoionization cross section $\sigma_{\rm PI}^{(B)}$.

The photorecombination cross section entering Eq. (27) is rarely measured directly. It is more common to derive it from the corresponding photoionization cross section of A^- using the *detailed balance principle* [1]. The latter is given as

$$k^2 g_A \sigma_{\rm PR}^{(A)}(\varepsilon) = k_{\rm ph}^2 g_{A^-} \sigma_{\rm PI}^{(A^-)}(\varepsilon), \tag{29}$$

where k and $k_{\rm ph}$ are the absolute values of the wave vectors of the captured electron and emitted photon, respectively, while g_A and g_{A^-} are the statistical weights of the quantum states of A and A^- [1].

Using the relation $E_{\rm vph} = \hbar k_{\rm vph} c$ we obtain the following working expression for the ICEC cross section

$$\sigma_{\rm ICEC}(\varepsilon) = \frac{3\hbar^4 c^2}{8\pi m_e} \frac{g_{A^-}}{g_A} \frac{\sigma_{\rm PI}^{(A^-)}(\varepsilon)\sigma_{\rm PI}^{(B)}(\varepsilon')}{\varepsilon R^6 E_{\rm vph}^2}. \tag{30}$$

It is this equation we intend to apply to some realistic systems in the next section.

The asymptotic formulas derived in this section for the case of a single neighbor can be generalized for the situation when the capturing center is surrounded by many neighbors. In this case the excess energy released in the capture event can be shed by ionizing any of the neighbors. If the distance between the latter is large enough so that one can neglect the interaction between them, the total ICEC cross section will be given by summing the cross sections corresponding to the different channels. Thus in the case of N equidistant identical neighbors the cross section in Eq. (27) should be multiplied by N [9]. In general only the nearest neighbors will make a noticeable contribution to the total cross section. However, even taking only them into account might increase the ICEC cross section by an order of magnitude. The same considerations apply to the results of the next subsection.

3. *ICEC into the excited virtual orbitals of atom A*

In the study of the photorecombination with atomic ions it is usually assumed that the free electron is predominantly captured into the lowest unoccupied orbital. The probability of its capture into the excited unoccupied orbitals decreases fast with the latter energies and is usually disregarded [4]. This conclusion does not necessarily remain valid in the case of ICEC due to the presence of the energy term in the denominator of Eq. (28). Indeed, while the photorecombination cross section in the numerator becomes smaller for the capture into the excited level, the concurrent decrease in the energy of the virtual photon might lead to an overall increase in the ICEC cross section.

We analyze this phenomenon in some detail by assuming that the atom A is a proton-like ion with the charge Z. Assuming the recombination to proceed to an excited state with the principal quantum number n and averaging over the orbital and magnetic quantum numbers one obtains the following

[1] In the previous letter [9] we erred by a factor 1/2 in the expression for the ICEC cross section.

quasiclassical expression for the photorecombination cross section [6]

$$\sigma_{\mathrm{PR}}^{(A)}(\varepsilon,n) = 1.96\pi^2 \frac{e^2\hbar}{m_e^2 c^3} \frac{E_1^2}{\varepsilon(\varepsilon+E_n)} n^{-3} \tag{31}$$

where ε is the kinetic energy of the incoming electron and $E_n = E_1/n^2$ is the energy necessary to remove an electron from the n-th level of $A^{(Z-1)+}$, or $V_n^{(A)}$ in our notation. This expression is valid near threshold, i.e., for ε being the order of magnitude of E_1 and breaks down for higher kinetic energies. Moreover, due to its quasiclassical nature, it is more accurate for higher n's. Near threshold this formula was found to overestimate the exact cross sections for lower n's [18]. However, the deviation for the kinetic energies of interest does not exceed 20%, and in the following analysis we are going to use this formula for all n's.

We introduce Eq. (31) into Eq. (28) and use the fact that the energy of the virtual photon given by $E_{\mathrm{vph}} = \varepsilon + E_n$. Neglecting the variation of $\sigma_{\mathrm{PI}}^{(B)}$ with energy we calculate the value of n such that the resulting $\sigma_{\mathrm{ICEC}}(\varepsilon)$ reaches its maximum at a given ε. One finds that $n_{\max}$ is given by the positive integer nearest to $(7E_1/3\varepsilon)^{1/2}$. If $V_i^{(B)}$ is the ionization potential of the neighboring species we may find the largest n_B such that $V_i^{(B)} < \varepsilon + E_1/n_B^2$. Thus, the ICEC channel will be open for electron capture into all levels with $n < n_B$. If $n_{\max} < n_B$, and neither $n_{\max}$ or n_B are equal to unity, we see that unlike in the photorecombination case, ICEC will predominantly proceed not to the ground state but rather to the state with $n = n_{\max}$. The conclusion remains true even if $n_B < n_{\max}$ in which case ICEC will predominantly proceed to the $n = n_B$. However, for the electron energies $\varepsilon \approx E_1$ the value of n_B approaches unity. This simple analysis demonstrates the importance of taking into account ICEC into excited unoccupied levels of A. This process can be the major contributor to the total ICEC cross section. We will see to what degree this assertion is correct for the examples of realistic systems studied later in the article.

B. Dielectronic ICEC

At electron energies just below an excitation energy of A, the incoming electron can be captured into a Rydberg state of A and lose its energy by exciting a bound electron of A. The resulting doubly excited resonance of A^- decays in an isolated system either by autoionization, i.e., re-emitting the electron back into the continuum and reverting to the original state of A, or by emitting a photon. In the latter case, called dielectronic recombination (DR) [7,8], the decay happens by relaxation of the excited "core" electron of A, while the electron in the Rydberg orbital remains a spectator. As a result, one obtains electronically excited A^- species in the final state. We note that the electronic capture through the dielectronic mechanism is usually possible only if A is a positive ion; for neutral A the excess electron in the final state will not be bound. In a medium an additional relaxation pathway can be added to the two mentioned above. The energy released in the relaxation of the excited core electron of A is transferred to a neighbor B ionizing it and producing again $(A^-)^*$ in the final state. The complete process, which we call dielectronic ICEC (dICEC), may be represented as occurring in two steps:

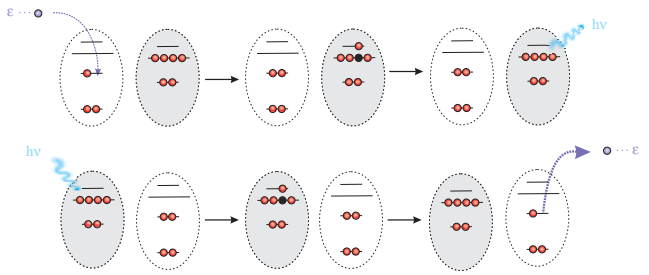

FIG. 3. (Color online) Schematic representation of the resonant ICEC and of the RICD processes. In resonant ICEC (upper drawing) the electron capture by one center is accompanied by an electron excitation of a neighboring species. The latter may relax through photon emission or any other relaxation mechanism. In the inverse process (lower drawing), a photon is absorbed, exciting an electron on one center. The resulting excited state decays by ionizing a neighboring species. This decay process is known as the resonant interatomic Coulombic decay (RICD) for inner-valence excitations or as excitation transfer ionization (ETI) for outer-valence excitations. The distinction between RICD and ETI is due to the fact that more decay channels become available following an inner-valence than following an outer-valence excitation.

dielectronic capture and interatomic decay of $(A^-)^{**}$, which are summarized in the following equation [see Fig. 1(c)],

$$e(\varepsilon) + A + B \rightarrow (A^-)^{**} + B \rightarrow (A^-)^* + B^+ + e(\varepsilon'). \tag{32}$$

The decay process in the second step of Eq. (32) belongs to the class of resonant interatomic Coulombic decay (RICD) processes. RICD has been previously the object of the experimental studies [10,11] and the detailed theoretical investigation of the underlying mechanisms is given in Ref. [12]. In an RICD process the initial inner-valence excitation, usually produced by absorbing a photon of corresponding energy, decays by transferring the energy and ionizing the environment (see Fig. 3). In the decay either the initially excited electron in a Rydberg orbital deexcites into the initial vacancy resulting in the *participator* process or one of the outer valence electrons resulting in the *spectator* process. The spectator process is usually by far the most efficient [12]. As we show under Sec. III, there are systems where dICEC can proceed through the inner-valence excited autoionizing states of $(A^-)^{**}$ in which case the second step in Eq. (32) is strictly a spectator RICD process. The incoming electron in the dICEC process can also be captured into an autoionizing resonance of $(A^-)^{**}$ where two outer valence electrons are simultaneously excited. The following interatomic decay where one of the electrons deexcites into the initial vacancy while another remains a spectator is closely related to RICD.

Our immediate task is to establish under what conditions dICEC is favored over DR. We assume that the cross section for the decay into any of the two channels above is given by the formula [14]

$$\sigma_{\mathrm{dICEC}} = \sigma_{\mathrm{DC}} \frac{\Gamma_{\mathrm{RICD}}}{\Gamma}, \quad \sigma_{\mathrm{DR}} = \sigma_{\mathrm{DC}} \frac{\Gamma_{\mathrm{ph}}}{\Gamma}, \tag{33}$$

where σ_{DC} is the cross section for the dielectronic capture, Γ_{RICD} and Γ_{ph} are the partial widths for the decay into the RICD or radiative channel, respectively. The total decay width $\Gamma = \Gamma_{\mathrm{ph}} + \Gamma_{\mathrm{RICD}} + \Gamma_{\mathrm{AI}}$, is the sum of the radiative, RICD,

and autoionization widths. We use the Breit-Wigner form for the cross section for dielectronic capture [4,14]

$$\sigma_{\mathrm{DC}} = \frac{C}{\varepsilon}\frac{g_d}{g_{\mathrm{in}}}\frac{A_{\mathrm{AI}}\Gamma}{(\varepsilon-\varepsilon_R)^2+\Gamma^2/4}, \tag{34}$$

where $\mathrm{A_{AI}} = \Gamma_{\mathrm{AI}}/\hbar$ is the autoionization rate, g_d is the weight of the decaying state, ε_R is the excess resonance energy obtained by subtracting from the resonance's energy E_R the ionization potential of A^-, and C is a numerical constant ($C = 7.88 \times 10^{-13}$ Mb eV^2 s [4]). We note here that the dielectronic capture is particularly effective for slow incoming electrons due to the factor ε in the denominator.

From Eqs. (33) and (34) we see that to estimate the relative importance of the resonance processes in question we need to know only their decay widths. The quantities Γ_{ph} and Γ_{AI} in Eqs. (33) and (34) can be understood as the radiative or autoionization widths of isolated $(A^-)^{**}$, and their values may be found in the literature. However, much less is known about the decay widths of the relatively unexplored interatomic processes. While numerical methods have been used [12] for calculating these widths, it has been also demonstrated that at large interatomic separations relevant for this article they can be reliably obtained using the virtual photon formulas [16,17]. In the virtual photon model of the interatomic decay, the excited $(A^-)^{**}$ species deexcites, emitting a virtual photon which is used to ionize B. The asymptotic expression for the RICD decay width averaged over the initial states is given by [12]

$$\Gamma_{\mathrm{RICD}} = \frac{3c^4\hbar^4}{4\pi}\frac{\sigma_{\mathrm{PI}}^{(B)}(\varepsilon)\Gamma_{\mathrm{ph}}}{E_{\mathrm{vph}}^4 R^6} \tag{35}$$

and is expressed through the parameters of the isolated excited species $(A^-)^{**}$ and the neighbor B, i.e., the radiative width Γ_{ph} of $(A^-)^{**}$ and the photoionization cross section $\sigma_{\mathrm{PI}}^{(B)}$ of B. Therefore, knowing the widths Γ_{ph} and Γ_{AI} together with the excited states energies of isolated species participating in the capture allows us to calculate both the σ_{dICEC} cross section and the ratio $\Gamma_{\mathrm{RICD}}/\Gamma_{\mathrm{ph}}$. Analyzing the latter we see that the conditions with respect to R, E_{vph}, and $\sigma^{(B)}$ under which dielectronic ICEC dominates over photon emission are similar to those in the case of ICEC.

We want to answer now the question of how the cross section of dICEC behaves, if there is N noninteracting neighbors near the capturing center. Increasing the number of neighbors available for RICD increases the probability of decay into this channel and correspondingly Γ_{RICD} at least N-fold. To see what changes it will produce in the dICEC cross section we consider two limiting cases. In the first one $N\Gamma_{\mathrm{RICD}} \ll \Gamma$, i.e., the decay into the RICD channel represents just a small proportion of all decay processes. Therefore, the N-fold increase in the RICD decay rate will lead according to Eqs. (33) and (34) to the N-fold growth in the intensity of the corresponding peak in the dICEC cross section, while its width will remain approximately constant. The area under the peak and the rate of the dICEC process will grow N-fold too, which indicates that RICD is the rate-limiting step in Eq. (32). In the second limiting case $\Gamma_{\mathrm{RICD}} \approx \Gamma$, i.e., almost all resonances formed in the dielectronic capture step will decay into the RICD channel. The N-fold increase in the RICD width will lead consequently to the approximately N-fold increase in the peak's width accompanied by the N-fold decrease in its intensity. The area under the peak and the rate of dICEC remain constant, indicating that dielectronic capture is the rate-limiting step of the whole process. One can also imagine a situation where increasing the number of neighbors will lead from one limiting case to another. Thus, when N is small the dICEC peak will grow as each new neighbor is added, until at some N the peaks' intensity will start to decrease while their widths' grow.

C. Resonant ICEC

The condition that the interatomic Coulombic capture involves the ionization of the surrounding medium can be extended to include the electronic excitation of the latter. In accordance with the nomenclature used in this article one can call such mechanism *resonant* ICEC. This extension is applicable to all three cases discussed above, namely capture to the ground state of A^-, to its excited states, and to dICEC. This resonant process is operative even when the excitation spectrum of the medium is discrete, in which case, only the electrons having the discrete values of energy corresponding to these excitations will be captured. We see immediately that this restriction essentially rules out the resonant dICEC in such media, because it is highly improbable that the energies of the autoionizing excited resonances in the intermediate state would coincide with the excitation energies of the medium. In a more interesting case of the media having a quasicontinuous electronic excitation spectrum, e.g., solutions, nanoparticles or solids, etc., the electrons having all values of energy in some interval can be captured. In the presence of such environment the resonant dICEC process becomes possible. In the final state of the capture the surrounding medium is electronically excited and can transfer the energy back to the capturing center ionizing it by the RICD mechanism discussed above. Therefore, it is important that the medium has alternative channels to shed this excitation energy. One of the ways is the photon emission, however, in complex media radiationless mechanisms such as vibronic coupling may have the upper hand.

In a recent publication Müller *et al.* [13] proposed and studied theoretically such a resonant interatomic capture mechanism which they called two center dielectronic recombination. In their case the excited species B stabilizes by emitting a photon and, therefore, this process can be summarized in the following equation

$$e(\varepsilon) + A + B \rightarrow (A^-) + B^* \rightarrow (A^-) + B + h\nu. \tag{36}$$

The authors have found that for specific electron energies the process can dominate photorecombination to distances up to several nanometers and that the two-center process is enhanced for smaller transferred energies.

We would like here to point to the relation the resonant ICEC process bears to the RICD process studied in the literature [10–12] and discussed above in Sec. IIB. In RICD an excited state of B is prepared and this excited state relaxes by transferring its energy to A and ionizing it. If this excited state of B is produced through photon absorption, the complete process, i.e., the photoabsorption and the decay by RICD, is

nothing but the inverse process of resonant ICEC; see Fig. 3. It can be summarized by the inverse of the equation Eq. (36): $h\nu + B + (A^-) \rightarrow B^* + (A^-) \rightarrow B + A + e(\varepsilon)$.

Analogous to the discussion in the previous subsection we write for its cross section assuming the Breit-Wigner form

$$\sigma_{\mathrm{RICD}} = \frac{\pi}{k_{\mathrm{ph}}^2}\frac{g_d}{g'}\frac{\Gamma_{\mathrm{ph}}\Gamma_{\mathrm{RICD}}}{(E_{\mathrm{ph}} - E_R)^2 + \Gamma^2/4}, \tag{37}$$

where E_{ph} is the energy of the absorbed photon and g' and g_d are the weights of the initial and the decaying states, while the rest of parameters have been defined previously. Applying the *detailed balance* equation Eq. (29) to the cross section in Eq. (37) we obtain for the cross section of the inverse process, i.e., the resonant ICEC process, the following expression:

$$\sigma = \frac{\pi}{k^2}\frac{g_d}{g_{\mathrm{in}}}\frac{\Gamma_{\mathrm{RICD}}\Gamma_{\mathrm{ph}}}{(\varepsilon - \varepsilon_R)^2 + \Gamma^2/4}, \tag{38}$$

which is exactly the cross section obtained in Ref. [13].

This elementary exercise provides an interesting example showing how different interatomic processes driven by electron correlation are interrelated. We also like to add at this point that if the photon absorption produces an inner-valence excitation of B, the decay process is named RICD in the literature, and if an outer-valence excited state of B is produced, the subsequent interatomic decay process is called excitation transfer ionization (ETI) [19]. The distinction is made due to the fact that additional interatomic channels become available in the case of inner-valence excited states [12]. In the above we use for brevity the term RICD for all cases.

We can imagine additional resonant ICEC processes and the corresponding interatomic decay processes related to them. Thus, resonant ICEC where the electron is captured into an excited state of A^- is related to the recently reported mechanism expected to be an important source of multiple ionization of clusters irradiated by intense laser source [20]. Under such conditions there is a large probability for an electronically excited species to be in a vicinity of an electronically excited neighbor. This leads to the interatomic decay with short lifetimes. For larger electron energies, inner-valence excitations of B can become possible. If the excited electron relaxes into the vacancy by emitting a photon the capture process will be the inverse of participator RICD discussed above. However, autoionization is often an efficient decay process, and the inner-valence excitation of B will decay also in this channel. The resulting capture process is then just the reverse of dICEC.

III. APPLICATION TO SELECTED SYSTEMS

We will now demonstrate the processes described above and compare them with each other for a number of realistic systems. To compute various ICEC cross sections using the derived asymptotic expressions several quantities such as energy levels, the photoionization cross sections, and the dielectronic capture cross sections must be available for the same system. These data are available in the literature only for very few systems and this dictated the choice of the systems we present here. We consider first the capture by Ne^+ in the presence of Xe and benzene (Bz). Another system is He^+ with Ar and Bz as its neighbors. Since the energies of the virtual photons are considerable in these systems, the values of the resulting ICEC cross sections are relatively small. Therefore, we considered also the interesting but probably an academic system Mg^+ with Br^- as its neighbor to show the dramatic enhancement the interatomic capture cross sections experience when the transferred energy is small.

A. Electron capture by Ne^+ with Xe and benzene as neighbors

We consider first the electron capture process by Ne^+ in its ground state in the presence of Xe and Bz species at interatomic distance of 1 nm. The spectroscopic information for neon is relatively abundant, and all data necessary to consider the processes discussed in the theoretical part are available in the literature. Moreover, neon is widely used in photoelectron experiments, which makes it a potential candidate for an experimental study of ICEC. We will discuss the photorecombination and ICEC into the ground and $2p^{-1}3p$ excited state of Ne. At the electron energies of interest, the recombination into the $2p^{-1}3s$, $2p^{-1}3d$ excited state of Ne is also possible. However, we consider these channels not to bring any new insights and omit them to avoid cluttering up the text and graphs.

The electron affinities of Ne^+ are $V_{\mathrm{gs}}^{(\mathrm{Ne}^+)} = 21.565$ eV and $V_{3p}^{(\mathrm{Ne}^+)} = 2.943$ eV [21], where the latter is averaged over all states of the configuration $2p^{-1}3p$. The photorecombination cross sections in Fig. 4 were obtained from the detailed balance equation in Eq. (29) using the photoionization cross section for the ground and excited $2p^{-1}3p$ states [22,23]. The latter cross section was averaged over all possible states belonging to the configuration $2p^{-1}3p$. The weight factors entering the calculations are, therefore, $g_{\mathrm{Ne}}^+ = 6$, $g_{\mathrm{Ne}} = 1$, and $g_{\mathrm{Ne}}(2p^{-1}3p) = 36$. We see that the photorecombination cross sections follow the expected order, with the photorecombination into the ground state being more probable than into an excited state. We compare them next to the ICEC cross sections (see Fig. 4) obtained from Eqs. (27) and (28) using the photoionization cross sections for Xe [23] and Bz [24]. Taking $V_i^{(\mathrm{Xe})} = 12.13$ eV and $V_i^{(\mathrm{Bz})} = 9.45$ eV, we see that the ICEC threshold for the capture into the ground state of Ne is at 0 eV for both neighbors and equals 9.19 and 6.51 eV for the capture into the Ne's $3p$ orbital for Xe and Bz as neighbors, respectively. Our first observation is that for both neighbors ICEC into the ground and in particular into the excited state prevails over photorecombination into the corresponding states in a range of electron energies above the respective ICEC thresholds. The second observation is that when both ICEC channels are open the capture proceeds largely into the excited state. Thus, for Xe as a neighbor the ratio of the respective cross sections at 11 eV is about 25, while for Bz it is $\approx$4 at 8 eV.

Let us now compare the ICEC cross sections of the two neighbors. The capture into the ground state at 5 eV is about 5 times more probable for Bz as a neighbor than for Xe. The capture into the excited state at 12 eV is still more probable in the case of Bz but the corresponding ratio is only 1.5. The difference in the efficiency of the ICEC mechanism for these two types of neighbors is due to the difference in the structure

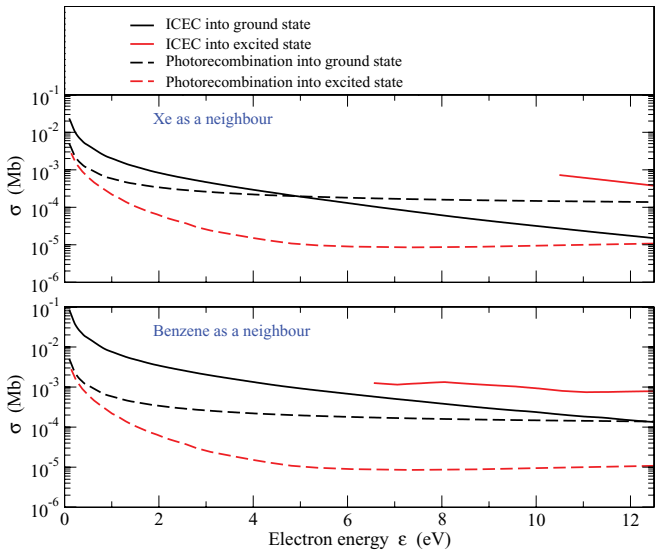

FIG. 4. (Color online) ICEC cross sections of Ne^+ computed using Eqs. (27) and (28). (Upper panel) Comparison of ICEC in Ne^+ with Xe as a neighbor with photorecombination in isolated Ne^+. Solid lines are the cross sections for ICEC into the ground state (lower curve; black) and into the $(2p^{-1}3p)$ excited state (upper curve; red) of Ne at the interatomic distance $R = 1$ nm. Dashed lines are the cross sections for photorecombination into the ground state (upper curve; black) and into the $(2p^{-1}3p)$ excited state (lower curve; red) of Ne. The experimental photoionization cross section of Xe reported in Ref. [23] starts at the threshold corresponding to Xe^+ $(^{1/2}P)$ which lies 1.3 eV above the lowest ionization potential corresponding to Xe^+ $(^{3/2}P)$. Therefore, the ICEC cross section for Ne^+ starts at 10.5 eV instead of 9.2 eV given in the text. (lower panel). Comparison of ICEC in Ne^+ with benzene as a neighbor with photorecombination in isolated Ne^+. The photoionization cross section of benzene averaged over orientation has been used in Eq. (28). The meaning of the various curves is as in the upper panel. The peak visible at 8 eV in the cross section for ICEC into the $(2p^{-1}3p)$ state derives from a pronounced peak in the photoionization cross section of Bz. Note the logarithmic scale.

of the photoionization cross sections of the Xe atom and the benzene molecule, the latter being on average larger for the virtual photon energies of interest. In addition, due to the lower ionization potential of Bz the threshold for the capture into the $3p$ orbital opens at lower kinetic energies of the incoming electron. Therefore, for energies between 6.51 and 9.19 eV the total ICEC cross section is more than one order of magnitude larger when benzene is the neighbor. The moment an additional capture channel for Xe opens[2] the corresponding cross sections begin to differ only by a factor of 1.3.

The absolute values of the ICEC cross sections for the electron energies considered are between 0.1 and 0.0005 Mb. Although larger than the cross sections for photorecombination, these absolute values are small compared to other processes present, e.g., excitations through electron collision. This is mostly due to the relatively large virtual photon energy. Under experimental conditions two factors might change the situation for a given system. First, the presence of several neighbors may increase the ICEC cross section by an order of magnitude. Second, according to Eq. (27), halving the interatomic distance will increase it by almost two orders of magnitude. Of course, other choices of the capturing center and/or of the neighbors can change the situation strongly.

We consider next the case of dielectronic capture in Ne^+ in the presence of Xe and Bz at the interatomic distance of 1 nm. The lowest energy optically allowed transition in Ne^+ is the excitation of the $2s$ electron to the $2p$ orbital at $E_{ph} = 26.91$ eV [21]. Thus, a free electron moving with an energy just below E_{ph} may excite the $2s$ electron and become captured in one of the Rydberg orbitals forming an autoionizing inner valence excited resonance state. These states form a number of series converging toward the threshold at E_{ph}. We chose for the study of dICEC the $2s^{-1}np\ ^1P^o$ series which has been studied both theoretically and experimentally [25,26]. The probability for the dielectronic capture is proportional to the autoionization width [see Eq. (34)] which for the series in question is given by $\Gamma_{AI} = \Gamma_{red}/n^{*3}$, where Γ_{red} is the reduced width and n^* is the effective quantum number. This width falls off with growing n, being about 12 meV at $n = 3$ and only 0.03 meV at $n = 20$. The partial width for photon emission in the intermediate state is $\Gamma_{ph} = 9.2$ μeV. Using Eq. (35) we also calculate the RICD widths at 1-nm interatomic distance, obtaining for Xe and Bz as neighbors 8.22 and 41.75 μeV, respectively. With these data we find the dICEC efficiency with Xe to be comparable to that of DR, while it is about four times more effective than DR with Bz as a neighbor.

The dICEC cross section is shown in Fig. 5. This cross section consists of a series of peaks corresponding to the capture into different autoionizing excited resonances. Their widths become progressively smaller, their intensities increase, and the area under the peaks remains constant as n rises and the autoionization width falls off. However, at some n where Γ_{AI} is small enough, the total width becomes nearly constant, since the radiative and RICD width are independent of n, and

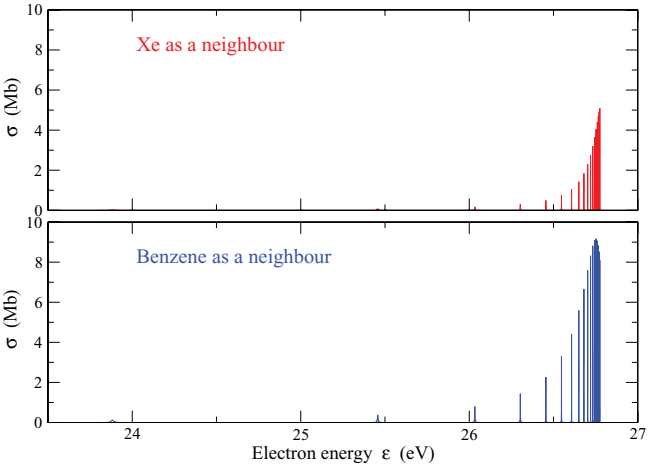

FIG. 5. (Color online) Dielectronic ICEC cross section of Ne^+ computed using Eqs. (33)–(35). (upper panel) Xe as a neighbor at the interatomic distance $R = 1$ nm. Intermediate states formed in the capture derive from $(2s^{-1}np)\ ^1P^o$ autoionizing excited states of Ne. (Lower panel) Same as in the upper panel but with benzene as a neighbor. The photoionization cross section of benzene averaged over orientation has been used in Eq. (35).

[2]We disregard the capture into the $3s$ orbital of Ne which makes negligible contribution to the total cross section.

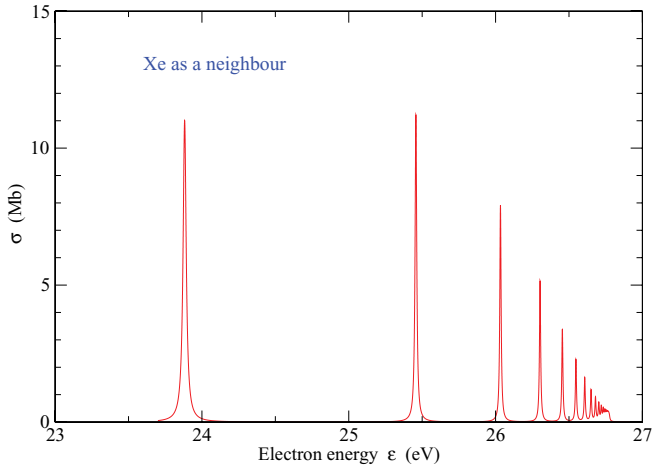

FIG. 6. (Color online) Dielectronic ICEC cross section of Ne^+ with Xe as a neighbor at an internuclear separation characteristic of a cluster computed using Eqs. (33)–(35). The RICD decay width is larger by a factor of 1000 than that for a distance of 1 nm shown in Fig. 5. Note the qualitatively different appearance of the cross section compared to Fig. 5 with more prominent peaks corresponding to the resonances with low quantum number n in the $(2s^{-1}np)\ ^1P^o$ autoionizing series of Ne.

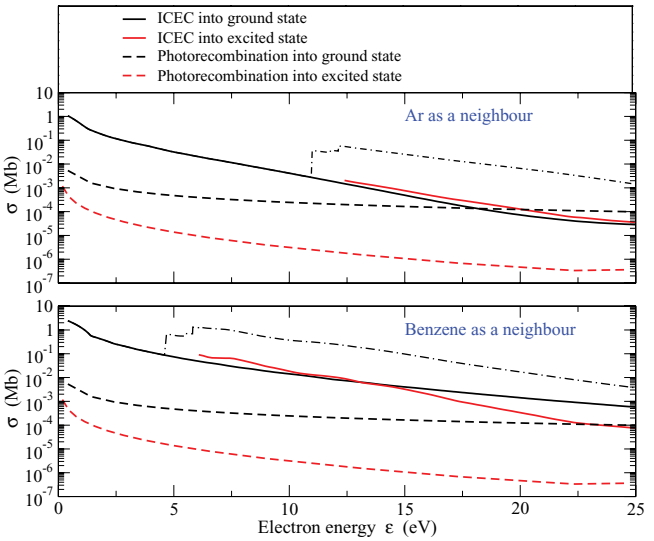

FIG. 7. (Color online) ICEC cross sections of He^+ computed using Eqs. (27) and (28). (Upper panel) Comparison of ICEC in He^+ with Ar as a neighbor with photorecombination in isolated He^+. Solid lines are the cross sections for ICEC into the ground state (lower curve; black) and into the $(1s^{-1}2p)\ ^1P^o$ excited state (upper curve; red) of He at the interatomic distance $R = 5$ Å. Dashed lines are the cross sections for photorecombination into the ground state (upper curve; black) and into the $(1s^{-1}2p)\ ^1P^o$ excited state (lower curve; red) of He. Dashed-dotted line is the total ICEC cross section for the capture into the $1s$, $2s$, and $2p$ orbitals. (Lower panel) Comparison of ICEC in He^+ with benzene as a neighbor with photorecombination in isolated Ne^+. The photoionization cross section of benzene averaged over orientation has been used in Eq. (28). The meaning of the various curves is as in the upper panel. Note that the curve for the ICEC cross section for the capture into the excited state intersects the one for the capture into the ground state at $\varepsilon = 13$ eV.

the intensities and the area of the peaks starts to decrease. This is well seen in the Ne^+ cross section with Bz as a neighbor where the peaks' maxima begin to decrease close to the end of the series. The intensity of the peaks in the respective cross section with Xe varies from 0.02 Mb for $n = 3$ to about 5 Mb for $n = 20$. Due to the difference in their respective RICD widths the low-lying peaks in the cross section with Bz have the same width but are about 5 times more intense than the corresponding peaks in the cross section with Xe. However, for larger n their intensity is only about factor 1.5 larger, while the peaks are about twice broader. Comparing Γ_{RICD} with Γ_{ph} we conclude that for Xe there is an equal probability for the intermediate state to decay by emitting a photon or ionizing a neighbor, while for Bz the latter process is about 4 times more probable.

Decreasing the interatomic distance or increasing the number of neighbors leads to a substantial increase in Γ_{RICD}. Although the asymptotic formulas are not expected to be valid at such distances, they provide a lower boundary for the cross sections, thus justifying their use at smaller distances [16]. Thus, in NeXe mixed cluster the interatomic distances are of the order of 3.5 Å, characteristic of bond lengths between rare gas atoms [27,28], and, according to Eq. (35), Γ_{RICD} can easily be three orders of magnitude larger than in the case of $R = 1$ nm discussed above. To visualize the corresponding change we show in Fig. 6 the dICEC cross section when $\Gamma_{\mathrm{RICD}} = 8.22$ meV. We see that the peaks have constant width but decreasing intensity as n grows. Contrary to the case considered above the largest intensity and area under the peak are observed for low n's.

B. Electron capture by He^+ with Ar and benzene as neighbors

Another system about which a wealth of information is available in the literature is the He atom. Therefore, we consider the interatomic capture by He^+ in the presence of Ar and Bz. As we have noted above, one of the reasons for the diminishing of the ICEC effectiveness in Ne^+ is the relatively large energy transferred in the process. This is even more the case for He^+. In what follows we offset the detrimental effect of large virtual photon energies by diminishing the interatomic distances to 0.5 nm. We would like to note that the interatomic distances between species in He nanodroplets used in studies of electron impact ionization [29,30] are of the order of a few Å.

We consider the interatomic capture in the $1s$, $2s$, and $2p$ orbitals of He^+ at $R = 0.5$ nm. As a result the following states of He can be formed in the capture: the ground state, and the ^1S, ^1P, ^3S, and ^3P excited states. The photoionization cross sections necessary to obtain the ICEC and photorecombination cross sections are given for He in Ref. [31], and for Ar and Bz in Refs. [22,24]. In Fig. 7 we show the resulting total ICEC cross section, and two partial cross sections corresponding to the capture into the ground state and into the $1s^{-1}2p\ ^1P$ state of He. The particular choice of the ^1P was dictated by the consideration that this state once formed may quickly relax by the RICD mechanism ionizing an additional neighbor. We see from Fig. 7 that ICEC dominates the photorecombination over a wide range of electronic energies. About the threshold at 0 eV the ICEC proceeds only to the ground state of He. The cross section with Ar is about 1 Mb at the threshold and

declines steadily until it reaches the value of 3×10^{-3} at about 11 eV. Additional interatomic capture channels open above 11 eV appearing as vertical jumps in the total ICEC cross section which becomes equal to 3.5×10^{-2} Mb at this threshold. A similar picture can be observed in the case of Bz where the cross section is about 2 Mb at 0 eV and decreases to about 0.1 Mb at 4.7 eV and jumps to 0.6 Mb once the next capture channel becomes available. We can also see from Fig. 7 that once the capture into the excited states becomes possible it proceeds predominantly into these states. The capture into the ^1P state is rather weak and comparable to the capture into the ground state. It is the capture into the triplet excited states ^3S, and ^3P which contributes most to the total ICEC cross sections.

At electron energies close to the $1s \rightarrow 2p$ transition of He^+ at 40.813 eV dielectronic processes become possible. Thus, the incoming electron can be captured into an np orbital with the simultaneous excitation of a $1s$ electron into the $2s$ orbital. Electron correlation mixes this $2snp\ ^1P^o$ series with the $2pns$ series, which has the same first member and converges to the same threshold [32]. Both theoretical and experimental values of the energies and autoionization widths of the so-called 20_n and 21_n series are given in Ref. [33]. The 20_n series is the strongest; its first four members ($n = 2, \ldots, 5$) are located between $\varepsilon = 35.5$ eV and $\varepsilon = 40.5$ eV and have the widths ranging from 37.4 to 1.8 meV. The three lowest members ($n = 2, \ldots, 5$) of the weaker 21_n series are located between $\varepsilon = 38$ and $\varepsilon = 40.5$ eV with corresponding widths between 0.105 and 0.027 meV. Again we note that the autoionization width and, hence, the probability of formation of these states falls off with increasing n.

The electron capture through these resonance states in the presence of neighbors proceeds again either by photon emission or RICD. The radiative width is $\Gamma_{\rm ph} = 6.6\ \mu$eV [34], while the RICD width is equal 11.8 μeV with Ar and 131.7 μeV with Bz as neighbors. These widths are correspondingly 2 and 20 times larger that the respective radiative one and, therefore, dICEC will be dominant capture mechanism. The corresponding cross sections are given in Fig. 8. We see that for the 20_n series $\Gamma_{\rm RICD} \ll \Gamma$ for both Ar and Bz as neighbors, therefore the peaks' amplitudes keep increasing as n increases and their widths diminish. The same is true for the 21_n series with Ar due to the rather small value of $\Gamma_{\rm RICD}$ in this case. In the 21_n series with Bz $\Gamma_{\rm RICD} \approx \Gamma$ and, therefore, we see that the peaks' intensity falls off as n increases. The maxima of the peaks for the 20_n series with Bz varies between 0.5 and 6 Mb, and with Ar the corresponding intensities are about 10 times weaker. The narrow peaks of the 21_n series vary between 7.5 and 20 Mb.

C. The unusual case of Mg^+ with Br^- as a neighbor

The large energy of the virtual photon transferred in the dielectronic capture of Ne^+ and He^+ with the neighbors studied is a main reason why the ICEC cross sections are relatively small. Generally, large virtual photon energies are due to large ionization potentials of the medium and/or large electron affinities of the capturing center. Also, in the case of dICEC large transition energies of the core electron in Ne^+ and He^+ led to smaller $\Gamma_{\rm RICD}$ and, consequently, decreased

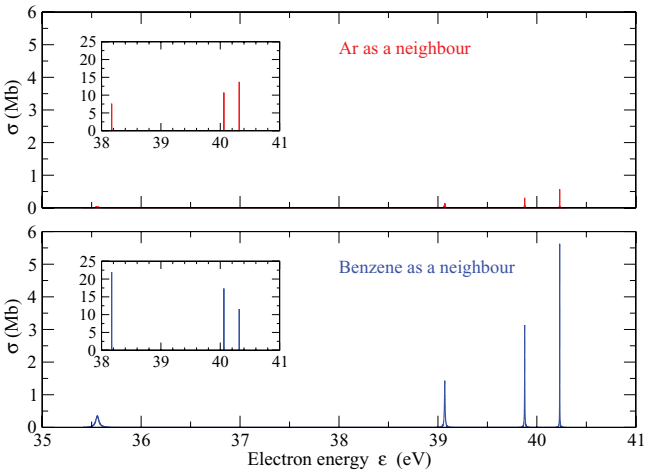

FIG. 8. (Color online) Dielectronic ICEC cross section of He^+ computed using Eqs. (33)–(35). (Upper panel) Ar as a neighbor at the interatomic distance $R = 5$ Å. The four peaks depicted in the graph correspond to the intermediate states belonging to the four lowest members of the $20_n\ ^1P^o$ doubly excited resonance series of He. The inset shows the peaks deriving from the intermediate states belonging to the three lowest members of the $21_n\ ^1P^o$ doubly excited resonance series of He. (Lower panel) Same as in the upper panel but with benzene as a neighbor. The photoionization cross section of benzene averaged over orientation has been used in Eq. (35).

the efficiency of dICEC. Larger electron energies needed to produce doubly excited resonances in these systems also result in diminished efficiency of the dielectronic capture [see Eq. (34)]. To demonstrate the effect of lower virtual photon energies on ICEC we consider the interatomic capture by Mg^+ with the environment modelled by Br^-.

The ionization potential of Br^- is 3.313 eV, and it has a comparatively large photoionization cross section of 10–40 Mb near threshold [35]. The ground state and $3s^{-1}3p\ ^1P$ excited state ionization energies of Mg give $V_{\rm gs}^{\rm Mg^+} = 7.646$ eV and $V_{3p}^{\rm Mg^+} = 3.3$ eV [21]. The corresponding photorecombination cross sections were obtained from the available ground state [36] and $3s^{-1}3p\ ^1P$ excited state [37] photoionization cross sections. The photoionization cross section from the excited state is more than the order of magnitude larger than the one from the ground state. This fact together with the relatively small difference between the energies of the ground and excited state leads to the very unusual situation that photorecombination into the excited state is more efficient than into the ground state, contrary to general theoretical expectations (see Fig. 9). In calculating the ICEC cross sections we have to correct the threshold energies for the mutual attraction of Mg^+ and Br^- in the initial state. At the interatomic distance of 1 nm the threshold energy remains zero for the ground state, while for the excited state this energy becomes 1.453 eV. The corresponding cross sections are given in Fig. 9. We see that the ICEC cross section remains larger than the unusually large photorecombination at the energies of interest. The effect of smaller transferred energies can be observed if we compare the cross sections in Fig. 9 with the capture by Ne^+ with neighbors in Fig. 4. The capture of slow electrons by Mg^+ is several times larger than by Ne^+ at the

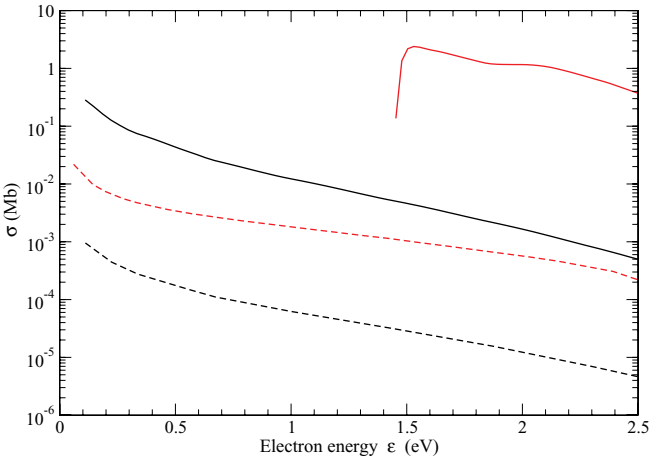

FIG. 9. (Color online) ICEC cross sections of Mg^+ computed using Eqs. (27) and (28). Comparison of ICEC in Mg^+ with Br^- as a neighbor at $R = 1$ nm with photorecombination in isolated Mg^+. Solid lines are the cross sections for ICEC into the ground state (lower curve; black) and into the $(3s^{-1}3p)\ ^1P^o$ excited state (upper curve; red) of Mg. Dashed lines are the cross sections for photorecombination into the ground state (lower curve; black) and into the $(3s^{-1}3p)\ ^1P^o$ excited state (upper curve; red) of Mg.

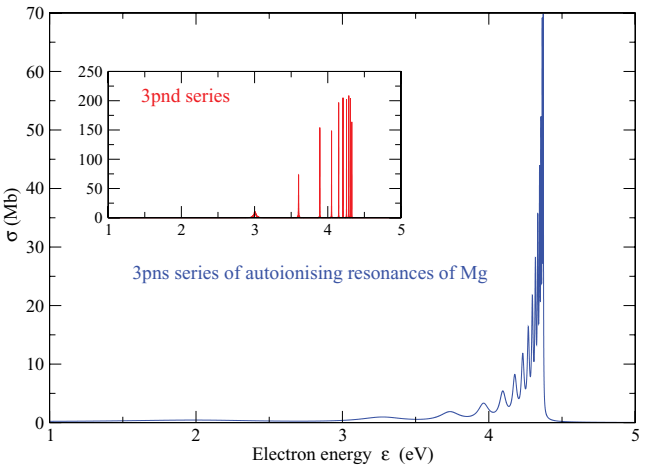

FIG. 10. (Color online) Dielectronic ICEC cross section of Mg^+ computed using Eqs. (33)–(35). The peaks in the main graph correspond to dICEC in Mg^+ with Br^- as a neighbor at $R = 1$ nm through the $3pns$ $(n = 4, \ldots, 18)\ ^1P^o$ series of doubly excited resonances of Mg. The inset shows the peaks corresponding to dICEC Mg^+Br^- at $R = 1$ nm through the $3pnd$ $(n = 3, \ldots, 12)\ ^1P^o$ series of doubly excited resonances of Mg.

same interatomic distance. At electron energies above 1.5 eV where the capture into the excited state become possible, the corresponding cross section is two orders of magnitude larger than the one for ICEC into the ground state and reaches the values as high as 2 Mb. This enhancement is due to both the smaller transferred energy and larger photorecombination cross section in the case of the excited state. Using the cross sections in Ref. [38] we can estimate that the cross section for the capture into excited states will further grow by 25%, if one includes the capture into the $3s^{-1}3p\ ^3P$ state.

We consider next the dICEC process in Mg^+ where the free electron is captured while the $3s$ electron of Mg^+ is excited into the $3p$ orbital. Two ^1P doubly excited resonance series converge to the $Mg^+(3p)$ threshold at 4.43 eV: $3pns$ and $3pnd$. In what follows we rely on the RPA calculations of the positions and widths of the corresponding terms [39] with $n =$ 4,. . .,18 in the $3pns$ case and $n = 3$,. . .,12 in the $3pnd$ case. Thus, in the $3pns$ series the positions between 2 and 4.4 eV with the corresponding autoionization widths being between 1200 and 2.9 meV. The weaker $3pnd$ series is located between 3 and 4.4 eV and has autoionization widths between 31 and 0.1 meV. The radiative width of these resonances is $\Gamma_{\rm ph} = 1.7 \times 10^{-4}$ meV [21], while the RICD width at $R = 1$ nm is 0.27 meV. We see that once the RICD channel is available one can neglect the photon emission altogether. The smaller energy of the virtual photon ensures that the RICD width here is larger than in Ne^+ with neighbors, though not as much as even an order of magnitude due to the almost two orders of magnitude difference between the radiative widths of Mg^+ and Ne^+ which enter Eq. (35) for $\Gamma_{\rm RICD}$. The dICEC cross sections corresponding to the series above are given in Fig. 10. For the stronger $3snp$ states we observe a series of peaks starting with a very broad one at 2 eV which converges to the ionization threshold at 4.43 eV. Since $\Gamma_{\rm RICD} \ll \Gamma$ for all states, these peaks become narrower, and their intensity grows, but their area remains approximately constant along the series. The peaks in this series are more pronounced than the peaks in the dICEC cross section of Ne^+ in Fig. 5, partly due to the larger $\Gamma_{\rm RICD}$ and partly due to the lower energies of incoming electrons. The weaker $2pnd$ resonances appear in the cross section as series of narrow pronounced peaks. Close to the $Mg^+(3p)$ threshold the intensity and area of these peaks begin to decrease, since $\Gamma_{\rm RICD} \approx \Gamma$. The dICEC cross section can become enormous as is demonstrated here. Other dramatic and more realistic examples can be anticipated, but the input data to compute the necessary cross sections is missing in the literature.

IV. CONCLUSIONS

In this article we considered the electron capture processes which become possible when the capturing center has neighbors and is particularly efficient when it is embedded in a medium of sufficient density. These processes, where the electron capture is accompanied by the ionization of a neighboring medium species, can be separated into two classes. The one where the electron capture and the medium's ionization happen in one step (ICEC) and the other where a resonance state is first formed on the capturing center which subsequently decays by ionizing the medium (dICEC). We derived the asymptotic formulas for the cross section of ICEC valid for large interatomic distances. Although similar in structure to analogous formulas developed for related interatomic processes, its derivation is more complicated due to the necessity to deal with the unbound electronic states both in the initial and final states of the process. To obtain the cross section of dICEC we included into the description of dielectronic capture an additional *interatomic* decay channel. The parameter of interest for this channel is the decay width which can be found from an asymptotic expression valid at large interatomic distances derived in earlier articles [16,17]. For each of the processes discussed one can anticipate the

related process where the neighbor or embedding medium is excited rather than ionized.

We considered the interatomic capture mechanisms in several model systems. We observed that for slow incoming electrons ICEC is more efficient than photorecombination for sizable interatomic distances. The dominance is most pronounces near the threshold of the ICEC channel and can reach orders of magnitude. The ICEC cross sections are very sensitive to the energy of the transferred virtual photon, increasing quickly when this energy becomes smaller. The energy of the virtual photon can be decreased by reducing the electron affinity of the capturing center (e.g., through the capture into an excited state), by lowering the ionization potential of the environment, or decreasing the energy of the incoming electron. We observed the corresponding change in the ICEC cross section when we compared the efficiency of the interatomic capture by Ne^+ and Mg^+, as well as into different electronic states in each of these systems separately. The cross section of ICEC depends strongly on the distance between the neighbors and falls off or increases quickly when the distance is increased or decreased. The efficiency of ICEC increases also with decreasing ionization potential of the surrounding medium as we could see for Ne^+ with the medium modelled either by Xe or by Bz. We found that under suitable conditions the ICEC cross sections may reach the respectable values of a few Mb at 1-nm interatomic distance. In the presence of several neighbors these values can grow by an order of magnitude.

The overall efficiency of dICEC is determined by the efficiency of the dielectronic capture and by the probability of the subsequent interatomic decay. The dielectronic capture is most efficient for slow electrons and for the capture into the low-lying excited states, while the probability of the interatomic decay behaves identically to ICEC with respect to the transferred energy, interatomic distance, and the photoionization cross section of the medium. Correspondingly, we have seen that the probabilities of dICEC at 1-nm interatomic distance and of the competing dielectronic recombination are similar in Ne^+ with Xe, while dICEC dominates with Bz as the neighbor which has a larger photoionization cross section. Moreover, dICEC by Mg^+ with Br^- is much more pronounced than by Ne^+ with Bz as a neighbor, due to the substantially lower transferred energy.

Although we mainly discussed the processes where the environment is ionized in the event of the electron capture we touched briefly on the alternative possibility of exciting the environment. While, as has been very recently demonstrated [13], resonant ICEC is possible even if the surrounding medium has a discrete electronic excitation spectrum, resonant dICEC can be observed only in the presence of the environment with a quasicontinuous electronic spectrum. The relation of resonant ICEC to known interatomic decay processes is demonstrated.

To conclude, we have described a fundamentally interatomic electron capture mechanism efficient in a medium with sufficient density and studied the conditions under which it will dominate its immediate competitors: photorecombination and dielectronic capture. Since ICEC and dICEC have been hardly studied so far, there is a need to search for potential applications of these processes. In this respect we hope that this work will stimulate other scientists.

[1] I. I. Sobel'man, *An Introduction to the Theory of Atomic Spectra* (Pergamon Press, Oxford, UK, 1972).

[2] E. Herbst, Nature (London) **289**, 656 (1981).

[3] D. E. Osterbrock and G. J. Ferland, *Astrophysics of Gaseous Nebulae and Active Galactic Nuclei*, 2nd ed. (University Science Books, Sausalito, CA, 2006).

[4] A. Müller, Adv. At. Mol. Opt. Phys. **55**, 293 (2008).

[5] M. Flannery, in *Springer Handbook of Atomic, Molecular, and Optical Physics*, edited by G. W. F. Drake (Springer, New York, 2006).

[6] H. A. Bethe and E. E. Salpeter, *Quantum Mechanics of One- and Two-Electron Atoms* (Dover, Mineola, NY, 2008).

[7] H. S. W. Massey and D. R. Bates, Rep. Prog. Phys. **9**, 62 (1943).

[8] R. H. Bell and M. J. Seaton, J. Phys. B **18**, 1589 (1985).

[9] K. Gokhberg and L. S. Cederbaum, J. Phys. B **42**, 231001 (2009).

[10] S. Barth, S. Joshi, S. Marburger, V. Ulrich, A. Lindblad, G. Öhrwall, O. Björneholm, and U. Hergenhahn, J. Chem. Phys. **122**, 241102 (2005).

[11] T. Aoto, K. Ito, Y. Hikosaka, E. Shigemasa, F. Penent, and P. Lablanquie, Phys. Rev. Lett. **97**, 243401 (2006).

[12] K. Gokhberg, V. Averbukh, and L. S. Cederbaum, J. Chem. Phys. **124**, 144315 (2006).

[13] C. Müller, A. B. Voitkiv, J. R. Crespo López-Urrutia, and Z. Harman, Phys. Rev. Lett. **104**, 233202 (2010).

[14] J. P. Taylor, *Scattering Theory* (Dover, Mineola, New York, 2006).

[15] F. Levin, Nucl. Phys. **46**, 275 (1963).

[16] V. Averbukh, I. B. Müller, and L. S. Cederbaum, Phys. Rev. Lett. **93**, 263002 (2004).

[17] K. Gokhberg, S. Kopelke, N. V. Kryzhevoi, P. Kolorenc, and L. S. Cederbaum, Phys. Rev. A **81**, 013417 (2010).

[18] L. H. Andersen, J. Bolko, and P. Kvistgaard, Phys. Rev. Lett. **64**, 729 (1990).

[19] K. Gokhberg, A. Trofimov, T. Sommerfeld, and L. S. Cederbaum, Europhys. Lett. **72**, 228 (2005).

[20] A. I. Kuleff, K. Gokhberg, S. Kopelke, and L. S. Cederbaum, Phys. Rev. Lett. **105**, 043004 (2010).

[21] Y. Ralchenko, A. E. Kramida, J. Reader, and NIST ASD Team (2008), NIST Atomic Spectra Database (version 3.1.5), online.

[22] J. Samson and W. Stolte, J. Electron Spectrosc. Relat. Phenom. **123**, 265 (2002).

[23] C. Duzy and H. A. Hyman, Phys. Rev. A **22**, 1878 (1980).

[24] R. Feng, G. Cooper, and C. Brion, J. Electron Spectrosc. Relat. Phenom. **123**, 199 (2002).

[25] K. Schulz, M. Domke, R. Püttner, A. Gutierrez, G. Kaindl, G. Miecznik, and C. H. Greene, Phys. Rev. A **54**, 3095 (1996).

[26] P. Lablanquie *et al.*, Phys. Rev. Lett. **84**, 431 (2000).

[27] P. Slavicek, R. Kalus, P. Paska, I. Odvarkova, P. Hobza, and A. Malijevsky, J. Chem. Phys. **119**, 2102 (2003).

[28] T. P. Haley and S. M. Cybulski, J. Chem. Phys. **119**, 5487 (2003).

[29] F. F. da Silva *et al.*, Phys. Chem. Chem. Phys. **11**, 11631 (2009).

[30] F. F. da Silva, P. Bartl, S. Denifl, O. Echt, T. D. Mark, and P. Scheier, Phys. Chem. Chem. Phys. **11**, 9791 (2009).

[31] V. L. Jacobs, Phys. Rev. A **9**, 1938 (1974).
[32] J. W. Cooper, U. Fano, and F. Prats, Phys. Rev. Lett. **10**, 518 (1963).
[33] M. Domke, K. Schulz, G. Remmers, G. Kaindl, and D. Wintgen, Phys. Rev. A **53**, 1424 (1996).
[34] J.-E. Rubensson, C. Såthe, S. Cramm, B. Kessler, S. Stranges, R. Richter, M. Alagia, and M. Coreno, Phys. Rev. Lett. **83**, 947 (1999).
[35] A. Mandl, Phys. Rev. A **14**, 345 (1976).
[36] M. Stener, G. D. Alti, G. Fronzoni, and P. Decleva, Chem. Phys. **222**, 197 (1997).
[37] M. Rafiq, S. Hussain, M. Saleem, M. A. Kalyar, and M. A. Baig, J. Phys. B **40**, 2291 (2007).
[38] T. K. Fang and T. N. Chang, Phys. Rev. A **61**, 052716 (2000).
[39] D.-S. Kim and S. S. Tayal, J. Phys. B **33**, 3235 (2000).